ELSEVIER

Journal of Molecular Catalysis B: Enzymatic 7 (1999) 147–156

JOURNAL OF MOLECULAR CATALYSIS B: ENZYMATIC

www.elsevier.com/locate/molcatb

Stabilisation centres differ between structurally homologous proteins as shown by NMR spectroscopy

Carlo P.M. van Mierlo *, Elles Steensma [1]

Department of Biomolecular Sciences, Laboratory of Biochemistry, Wageningen Agricultural University, Dreijenlaan 3, NL-6703 HA Wageningen, The Netherlands

Abstract

The local stabilities of apo- and holoflavodoxin from *Azotobacter vinelandii* as probed by hydrogen/deuterium exchange measurements and nuclear magnetic resonance (NMR) spectroscopy are discussed. Residues in strands β1, β3, β4 and β5a and in helices α4 and α5 of apoflavodoxin form its stability centre. Upon binding of the flavin cofactor, large parts of the conformation of the molecule remain unaltered. However, a significant increase of the local stabilities of the majority of the residues and an extension of the stability centre of holoflavodoxin, as compared to that of apoflavodoxin, are observed. The corresponding amide proton exchange rates can decrease more than 10,000 times. This is most likely caused by a shift in the equilibria between the various substates of the protein towards its fully folded native state. Both Che Y and cutinase, which have no sequence homology with apoflavodoxin but which share the flavodoxin-like topology, have stabilisation centres different from that of apoflavodoxin. The stable centres of structurally homologous proteins can thus reside in different parts of the same protein topology. Insight in the variations in (local) unfolding processes of structurally homologous proteins can be used to stabilise proteins with a flavodoxin-like fold.

Keywords: Apoflavodoxin; Holoflavodoxin; Hydrogen/deuterium exchange; Protein stability; Protein folding; NMR spectroscopy; Ligand-binding

1. Introduction

Due to the presence of two main elements of secondary structure (being a β-sheet surrounded by α-helices) a flavodoxin was chosen by us as a model system to study protein folding and stability. In contrast to most protein folds, the flavodoxin-like fold is shared by many (i.e., nine) superfamilies [1]. These nine superfamilies exhibit little or no sequence similarity and comprise a broad range of unrelated proteins with different functions like catalases, chemotactic proteins, lipases, esterases and flavodoxins. They are all characterised by a five-stranded parallel β-sheet surrounded by α-helices at either side of the sheet (Fig. 1). Studies on these structurally but not sequentially related proteins are pre-eminently suitable to study protein folding and stability.

Flavodoxins are a group of small flavoproteins which function as low-potential one-electron carriers and contain a non-covalently bound FMN cofactor [2]. The protein investi-

* Corresponding author. Tel.: +31-317-484621; Fax: +31-317-484801; E-mail: carlo.vanmierlo@nmr.bc.wau.nl

[1] Current address. Department of Biochemistry, Uppsala University, Box 576, S-75123 Uppsala, Sweden.

1381-1177/99/$ - see front matter
PII: S1381-1177(99)00037-5

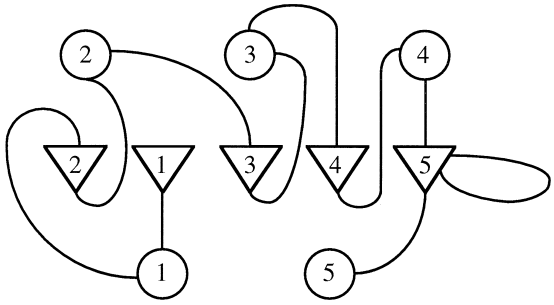

Fig. 1. Topology of the flavodoxin-like fold: α-helices are represented as circles, β-strands as triangles and loops as lines. Note that a long loop (> 20 residues) interrupts β-strand 5; this loop is absent in short-chain flavodoxins.

gated by us is flavodoxin II from *Azotobacter vinelandii* (strain ATCC 478), henceforth designated as flavodoxin. Its gene has been cloned in *Escherichia coli* and brought to high expression in our laboratory. The protein consists of 179 amino acid residues and belongs to the class of 'long-chain' flavodoxins [3]. Upon removal of the flavin, apoflavodoxin is generated. The characterisation of the apoform of the protein is required to be able to compare the inherent structure and inherent stability of flavodoxin with those of members of superfamilies sharing the flavodoxin-like fold. Apoflavodoxin molecules were shown to rapidly dimerise via the formation of an intermolecular disulphide bond involving the sole cysteine residue at position 69. To avoid this complication, the single cysteine residue was replaced by an alanine residue [4].

Detailed knowledge about the conformational properties of a protein is a prerequisite to study its folding and stability. The good nuclear magnetic resonance (NMR) characteristics of flavodoxins (solubility, relatively narrow linewidths) allow a detailed structural characterisation of these proteins in solution [5,6] using a variety of heteronuclear multidimensional NMR experiments (see, e.g., Refs. [7,8]). As a result, ^{1}H, ^{13}C and ^{15}N backbone chemical shifts of the electron carrier, holoflavodoxin [6], and ^{1}H and ^{15}N backbone chemical shifts of apoflavodoxin [9] could be determined using multidimensional NMR spectroscopy. The NMR results show that flavodoxin contains a five-stranded parallel β-sheet (order β2–β1–β3–β4–β5) and five α-helices in both the holo- and apoform. Despite the removal of the FMN cofactor, large parts of the tertiary structure of holo- and apoflavodoxin are strictly conserved as is reflected in the identity of their chemical shifts (Fig. 2). Native apoflavodoxin has a stable well-ordered core but in contrast to holoflavodoxin, its flavin binding region is shown to be flexible [9]. Using the hydrogen exchange method and NMR spectroscopy, exchange rates for the individual amide protons of apo- and holoflavodoxin were measured [6,9]. The exchange rates relate to local free energies for transient opening of protein structures [10] and therefore, local stabilities of apo- and holoflavodoxin could be determined.

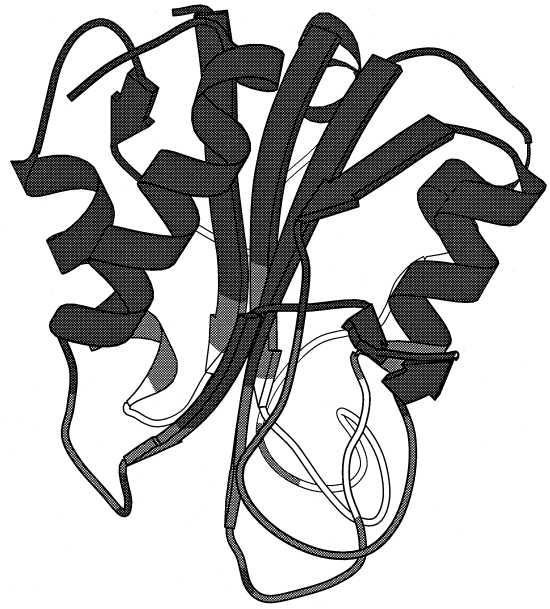

Fig. 2. Molscript cartoon drawing [21] of the X-ray structure of *Azotobacter chroococcum* flavodoxin [22]. The structure is grey-colored according to the ^{1}Hα chemical shift differences ($\Delta\delta$) between the holo- and the apoform of the highly homologous *A. vinelandii* apoflavodoxin [9]. The length of the α-helices and of the β-strands shown in the global fold of apoflavodoxin is determined by the NMR data [9]. Dark grey: $\Delta\delta \leq 0.1$ ppm; light grey: $\Delta\delta > 0.1$ ppm; white: residues of which the ^{1}Hα proton could not be assigned. Dynamic exchange between different conformations occurs in the flavin-binding region of the molecule which is colored light grey and white.

In this paper, we discuss the local stabilities of apo- and holoflavodoxin as measured by NMR spectroscopy. We define the stabilisation centre as the most stable part of a protein topology which consists of one or more secondary structure elements. The stabilisation centres of apo- and holoflavodoxin are presented. The local stabilities of apo- and holoflavodoxin are mutually compared and the effects of the incorporation of the flavin cofactor on the properties of the apoprotein are discussed. The stabilisation centre of apoflavodoxin is compared with those of proteins sharing the flavodoxin-like fold. Among these proteins are the chemotactic protein, Che Y, and the lipolytic enzyme, cutinase. It is shown that the stabilisation centres differ among these three structurally homologous proteins and the use that can be made hereof is discussed.

2. Experimental

2.1. Materials

Uniformly ^{15}N-labelled recombinant *A. vinelandii* C69A holoflavodoxin II (strain ATCC 478) was obtained and purified as described previously [6]. By trichloroacetic acid precipitation according to a slightly modified version [11] of the original procedure [12], apoflavodoxin was generated. The enzymes used for cloning and the chemicals used were purchased from the companies as described in Ref. [11].

2.2. NMR spectroscopy and data analysis

In the hydrogen/deuterium exchange measurements, lyophilised apo- and holoflavodoxin were reconstituted in 99.9% $^{2}H_2O$, at 303 K. ^{1}H–^{15}N HSQC experiments were carried out on a Bruker AMX-500 spectrometer and are described in Refs. [6,9]. The NMR data were referenced, processed and analysed as described previously [6,9]. Peak intensities were measured and subsequently, a single exponential decay function (Eq. (1)) was fitted to the time-dependent cross-peak intensities, using Kaleidagraph version 2.1.3. (Adelbeck, Synergy Software, Reading, PA, USA), to determine the amide proton exchange rate, k_{ex}:

$$I(t) = I(\infty) + I(0) * \exp(-k_{ex} t), \qquad (1)$$

with t, the time between the addition of $^{2}H_2O$ to the lyophilised apoflavodoxin and the beginning of each individual ^{1}H–^{15}N HSQC experiment; $I(0)$, the cross-peak intensity at time zero and $I(\infty)$, the cross-peak intensity at the infinity time point. For amide protons, that did not exchange completely within the experiment and for which the infinity time-point was not well-determined, the decay curve was fitted using a final intensity of zero.

2.3. Local stability determination

Hydrogen exchange rates can be analysed in terms of a structural unfolding model, in which exchange only takes place from an 'open' (exchange-competent) form of the protein, but not from the 'closed' (exchange-incompetent) form:

$$\text{N–H (closed)} \underset{k_f}{\overset{k_u}{\rightleftarrows}} \text{N–H (open)} \xrightarrow{k_{int}} \text{N–D}, \qquad (2)$$

with k_u and k_f as the local unfolding and folding rates, respectively, and k_{int}, the intrinsic exchange rate of an amide proton in the open form [13,14]. The sequence-specific intrinsic exchange rates for an amide proton, k_{int}, can be calculated for each protein [15]. In the EX2 limit (bimolecular reaction), which is the dominant mechanism of exchange for most proteins at moderate pH and temperature, $k_f \gg k_u$ and $k_f \gg k_{int}$. The measured exchange rate, k_{ex}, can therefore be written as:

$$k_{ex} = k_u k_{int}/k_f = K_{op} k_{int}, \qquad (3)$$

where K_{op} is the equilibrium constant for local transient opening of a hydrogen-bonded site. This equilibrium constant relates to ΔG_{op}, the

local free energy difference between the closed and open states:

$$\Delta G_{op} = -RT \ln K_{op} = -RT \ln(k_{ex}/k_{int}), \quad (4)$$

with R, the gas constant and T, the absolute temperature. The protection factor P is calculated according to:

$$P = k_{int}/k_{ex}. \quad (5)$$

Using the measured exchange rates, k_{ex}, and the intrinsic chemical exchange rates, k_{int}, the local stability differences for individual amide protons ΔG_{op}, were determined.

3. Results and discussion

3.1. Hydrogen exchange kinetics and local stability of apoflavodoxin

For 57 amide protons of ^{15}N-labelled apoflavodoxin, a single exponential function (Eq. (1)) could be fitted to the time-dependent cross-peak intensities to determine their exchange rates, k_{ex} [9]. As an example, the decrease in cross-peak intensity with time of the backbone NH proton of Val142 in apoflavodoxin is shown in Fig. 3A. The amide proton exchanges relatively rapidly, $k_{ex} = 4.65\ 10^{-4}$ s^{-1}. This corresponds with a local stability of 3.7 kcal mol^{-1}, using Eq. (4) and the corresponding k_{int} value from Ref. [15]. Likewise, the local stability differences for the remaining individual amide protons of apoflavodoxin were obtained (see Table 1).

Fig. 4A shows the global fold of apoflavodoxin grey-shaded according to the calculated local stability differences for transient opening of the structure. The slowest exchanging amide protons reside in the ordered core of apoflavodoxin and form its stabilisation centre, whereas amide protons in the flexible flavin-binding region exchange rapidly. The stabilisation centre of apoflavodoxin comprises roughly 28 residues in strands β1, β3, β4 and β5a and in helices α4 and α5. Strand β5a is part of β-strand 5

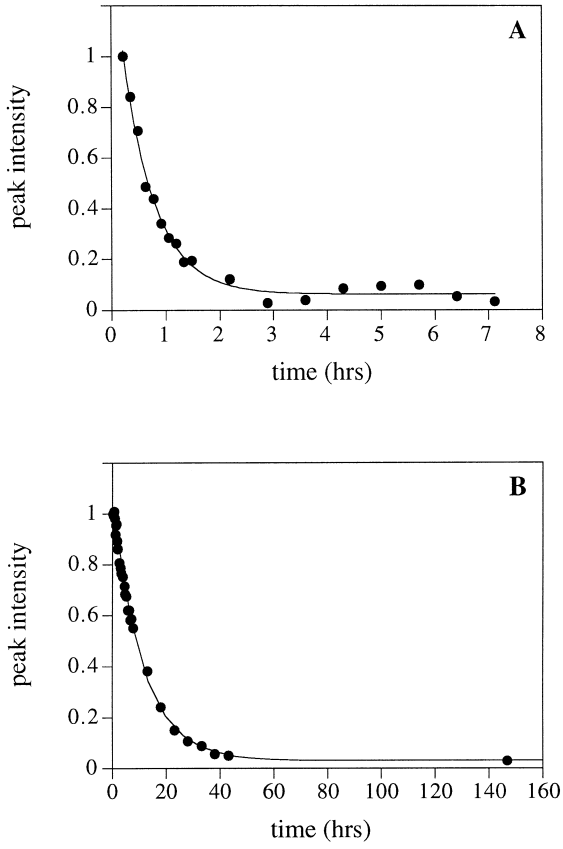

Fig. 3. Time-dependent decrease in ^{1}H–^{15}N HSQC cross-peak intensity of the backbone amide proton of Val142 after transfer of apoflavodoxin (A) and holoflavodoxin (B) from *A. vinelandii* in 99.9% $^{2}H_2O$. Intensities were normalised to the intensity of the first data point. The solid line is a least-squares fit of a single exponentially decaying function (Eq. (1)) to the data with $k_{ex} = 4.65\ 10^{-4}\ s^{-1}$ for apoflavodoxin and with $k_{ex} = 2.45\ 10^{-5}\ s^{-1}$ for holoflavodoxin.

and is at the N-terminal side of the 23-residue loop insertion which is characteristic for long-chain flavodoxins. This loop separates strands β5a and β5b.

Exchange of the amides in the stabilisation centre is expected to occur via global unfolding of the protein. The average local stability of the stabilisation centre should, therefore, approximate the global stability of apoflavodoxin. Its average ΔG_{op} value is calculated to be 7.0 kcal mol^{-1} (Table 1). The extremely slow exchange of the backbone amide protons of Tyr114, Phe117, and Lys118 is most likely caused by

residual structure in the aromatic region Y_{114}–S–F–F–K_{118} of the unfolded state of the protein [9]. Consequently, the local stability values obtained for Tyr114, Phe117, and Lys118 are remarkably high (> 8.2 kcal mol^{-1}) and were not used in the calculation of the global stability of apoflavodoxin.

3.2. Comparison of the local stabilities of apoflavodoxin with those of holoflavodoxin

In the case of holoflavodoxin, strikingly decreased amide proton exchange rates, as compared to the corresponding exchange rates of apoflavodoxin, are observed (Table 1). This is illustrated for the backbone NH proton of Val142 in Fig. 3B. The exchange rate, k_{ex}, equals 2.45 10^{-5} s^{-1} in holoflavodoxin, which leads to a local stability of 5.5 kcal mol^{-1}. The amide proton of Val142, therefore, exchanges 19 times slower with the solvent in holoflavodoxin as in apoflavodoxin.

A summary of the hydrogen exchange results on 4.3 mM holoflavodoxin [6] is shown in Fig. 4B which is grey-shaded according to the calculated local stability differences for transient opening of the holoflavodoxin structure. The stabilisation centre of holoflavodoxin, characterised by $\Delta G_{op} \geq 6.2$ kcal mol^{-1}, contains roughly 70 amino acid residues including the residues which form the stabilisation centre in apoflavodoxin. Clearly, in holoflavodoxin, the region with high local stability values is extended as compared to apoflavodoxin (Fig. 4). The amide protons of 54 of these 70 amino acid residues had not exchanged in the 42-h exchange experiment involving holoflavodoxin and consequently, the ΔG_{op} of these residues was estimated to be $\geq \sim 9.5$ kcal mol^{-1} [6]. This is significantly higher than the average ΔG_{op} value of 7.0 kcal mol^{-1} found for the residues which are part of the stabilisation centre of apoflavodoxin. The hydrogen exchange results thus show that apoflavodoxin is substantially less stable than holoflavodoxin as is confirmed by denaturant and temperature-induced equilibrium unfolding studies (data not shown).

Upon binding of the flavin, large parts of the conformation of the apoflavodoxin molecule remain unaltered (Figs. 2 and 4). The amino acid residues in the flavin-binding region of the protein, however, no longer exhibit the considerable conformational dynamics as observed in apoflavodoxin. In contrast with apoflavodoxin, several residues in the flavin-binding region of the molecule (Fig. 4B) exchange extremely slowly in holoflavodoxin ($\Delta G_{op} \geqslant \sim 9.5$ kcal mol^{-1}). This reflects the rigidity of the flavin-binding region in holoflavodoxin which is caused by the many interactions that exist between the non-covalently bound FMN cofactor and the apoprotein.

Residue Val142 discussed above resides in the 23-residue loop which is characteristic for long-chain flavodoxins. This loop is structurally well-defined and packed onto the remainder of the molecule in essentially the same way in both apo- and holoflavodoxin as is inferred from the extensive NMR data on both protein molecules [6,9]. The time-averaged conformation of this part of the molecule must therefore be virtually indistinguishable between native apo- and holoflavodoxin. The hydrogen exchange results, however, imply that the sampling of the various conformational substates, including the unfolded states, of this part of the molecules differs significantly. The linewidths of most cross-peaks arising from amide groups of the ordered part of the apoprotein are essentially identical to those of the holoprotein [9]. Consequently, the processes which affect the hydrogen exchange rates must take place on a timescale which exceeds the millisecond time range. Hydrogen exchange measurements have the advantage of being able to detect motions on such relatively large timescales. The remarkable decrease in amide proton exchange rates upon going from the apo- to the holoform of the protein is most likely caused by a shift in the equilibria among the various substates of the protein towards the fully folded native state

Table 1
Amide proton exchange rates (k_{ex}) and calculated local free energy differences [ΔG_{op} (298 K)] of *Azotobacter vinelandii* apo- and holoflavodoxin in 150 mM potassium pyrophosphate, pH* 6.2, at 303 K

Residue		Apo k_{ex} (s^{-1})	Holo k_{ex} (s^{-1})	Apo ΔG_{op} (kcal mol^{-1})	Holo ΔG_{op} (kcal mol^{-1})
1	Ala	–	–	–	–
2	Lys	–	–	–	–
3	Ile	–	5.97e−06	–	6.61
4	Gly	–	1.00e−07	–	9.54
5	Leu	1.32e−05	1.00e−07	6.42	9.54
6	Phe	1.04e−05	1.00e−07	6.51	9.54
7	Phe	–	1.00e−07	–	9.54
8	Gly	6.87e−04	1.00e−07	5.09	9.54
9	Ser	–	–	–	–
10	Asn	–	1.00e−02	–	1.36
11	Thr	–	1.00e−02	–	1.36
12	Gly	–	–	–	–
13	Lys	–	1.07e−03	–	4.55
14	Thr	–	9.07e−06	–	7.27
15	Arg	–	1.00e−07	–	9.54
16	Lys	–	1.12e−06	–	8.69
17	Val	2.29e−04	1.00e−07	4.50	9.54
18	Ala	9.08e−05	1.00e−07	5.65	9.54
19	Lys	7.84e−05	1.00e−07	5.87	9.54
20	Ser	–	–	–	–
21	Ile	4.76e−05	1.00e−07	5.64	9.54
22	Lys	4.72e−05	1.00e−07	5.86	9.54
23	Lys	–	1.21e−05	–	7.15
24	Arg	1.55e−03	8.77e−04	4.43	4.77
25	Phe	–	1.15e−05	–	7.04
26	Asp	1.00e−02	1.00e−02	1.36	1.36
27	Asp	–	–	–	–
28	Glu	1.00e−02	1.00e−02	1.36	1.36
29	Thr	1.00e−02	1.00e−02	1.36	1.36
30	Met	–	1.37e−04	–	5.85
31	Ser	1.00e−02	1.71e−03	1.36	4.76
32	Asp	1.00e−02	1.00e−02	1.36	1.36
33	Ala	1.00e−02	2.55e−03	1.36	3.61
34	Leu	–	1.00e−07	–	9.54
35	Asn	–	1.00e−02	–	1.36
36	Val	–	–	–	–
37	Asn	–	1.49e−04	–	6.03
38	Arg	–	3.16e−03	–	4.28
39	Val	–	5.23e−04	–	4.15
40	Ser	–	1.00e−02	–	1.36
41	Ala	1.00e−02	1.00e−02	1.36	1.36
42	Glu	1.00e−02	1.00e−02	1.36	1.36
43	Asp	8.98e−04	–	3.87	–
44	Phe	–	–	–	–
45	Ala	9.13e−05	7.69e−05	5.92	6.01
46	Gln	1.39e−03	3.13e−03	4.31	3.83
47	Tyr	1.66e−04	–	5.39	–
48	Gln	1.00e−02	1.00e−02	1.36	1.36
49	Phe	1.93e−05	1.49e−05	6.70	6.86
50	Leu	1.57e−06	1.00e−07	7.53	9.54

Table 1 (continued)

Residue		Apo k_{ex} (s^{-1})	Holo k_{ex} (s^{-1})	Apo ΔG_{op} (kcal mol^{-1})	Holo ΔG_{op} (kcal mol^{-1})
51	Ile	1.35e−06	1.00e−07	7.05	9.54
52	Leu	2.00e−06	1.00e−07	6.99	9.54
53	Gly	1.97e−05	1.00e−07	6.83	9.54
54	Thr	–	1.00e−07	–	9.54
55	Pro	–	–	–	–
56	Thr	–	1.00e−07	–	9.54
57	Leu	–	1.48e−03	–	3.67
58	Gly	–	2.89e−03	–	3.87
59	Glu	–	1.00e−02	–	1.36
60	Gly	–	1.96e−03	–	4.19
61	Glu	–	1.09e−03	–	3.90
62	Leu	–	3.35e−03	–	2.71
63	Pro	–	–	–	–
64	Gly	–	5.36e−03	–	3.46
65	Leu	–	4.43e−03	–	2.97
66	Ser	–	1.00e−02	–	1.36
67	Ser	–	1.00e−02	–	1.36
68	Asp	1.00e−02	1.00e−02	1.36	1.36
69	Ala	1.00e−02	–	1.36	–
70	Glu	1.00e−02	1.00e−02	1.36	1.36
71	Asn	–	1.33e−03	–	4.72
72	Glu	–	1.00e−02	–	1.36
73	Ser	–	4.98e−04	–	5.13
74	Trp	1.00e−02	4.21e−04	1.36	4.79
75	Glu	–	4.96e−04	–	4.00
76	Glu	–	3.47e−05	–	5.51
77	Phe	–	1.00e−07	–	9.54
78	Leu	–	–	–	–
79	Pro	–	–	–	–
80	Lys	1.26e−04	1.68e−05	5.27	6.46
81	Ile	5.93e−06	1.00e−07	6.62	9.54
82	Glu	7.44e−05	2.57e−05	4.95	5.58
83	Gly	1.00e−02	1.00e−02	1.36	1.36
84	Leu	8.31e−05	5.61e−05	5.33	5.56
85	Asp	–	–	–	–
86	Phe	1.00e−02	–	1.36	–
87	Ser	–	–	–	–
88	Gly	1.00e−02	1.00e−02	1.36	1.36
89	Lys	–	5.55e−06	–	7.68
90	Thr	1.81e−05	1.00e−07	6.86	9.54
91	Val	3.08e−06	1.00e−07	7.16	9.54
92	Ala	3.32e−06	1.00e−07	7.61	9.54
93	Leu	2.14e−06	1.00e−07	7.27	9.54
94	Phe	2.14e−06	1.00e−07	7.45	9.54
95	Gly	1.00e−04	1.00e−07	6.23	9.54
96	Leu	–	1.00e−07	–	9.54
97	Gly	5.34e−04	–	4.87	–
98	Asp	–	1.00e−07	–	9.54
99	Gln	1.00e−02	1.00e−07	1.36	9.54
100	Val	1.97e−03	1.00e−07	3.34	9.54
101	Gly	1.00e−02	5.29e−06	1.36	7.70
102	Tyr	1.00e−02	1.00e−07	1.36	9.54
103	Pro	–	–	–	–
104	Glu	1.00e−02	1.00e−02	1.36	1.36

Table 1 (continued)

Residue		Apo k_{ex} (s^{-1})	Holo k_{ex} (s^{-1})	Apo ΔG_{op} (kcal mol^{-1})	Holo ΔG_{op} (kcal mol^{-1})
105	Asn	1.00e−02	2.04e−04	1.36	5.82
106	Tyr	–	1.00e−07	–	9.54
107	Leu	–	1.00e−07	–	9.54
108	Asp	–	1.00e−07	–	9.54
109	Ala	–	–	–	–
110	Leu	5.46e−05	1.00e−07	5.35	9.54
111	Gly	2.94e−05	1.00e−07	6.59	9.54
112	Glu	–	6.15e−04	–	4.24
113	Leu	4.90e−05	1.00e−07	5.21	9.54
114	Tyr	1.00e−07	1.00e−07	9.54	9.54
115	Ser	–	6.54e−06	–	7.98
116	Phe	–	1.66e−06	–	8.29
117	Phe	1.00e−07	1.00e−07	9.54	9.54
118	Lys	1.94e−06	–	8.15	–
119	Asp	9.23e−04	9.29e−04	4.22	4.21
120	Arg	1.18e−05	–	6.91	–
121	Gly	1.00e−02	1.00e−02	1.36	1.36
122	Ala	–	–	–	–
123	Lys	1.39e−05	6.31e−06	6.90	7.36
124	Ile	1.00e−02	3.48e−03	1.36	2.85
125	Val	2.95e−06	1.00e−07	6.60	9.54
126	Gly	1.00e−02	1.00e−02	1.36	1.36
127	Ser	1.00e−02	1.00e−02	1.36	1.36
128	Trp	6.10e−04	2.39e−06	4.56	7.84
129	Ser	1.00e−02	1.00e−02	1.36	1.36
130	Thr	1.00e−02	–	1.36	–
131	Asp	1.00e−02	6.61e−03	1.36	3.16
132	Gly	1.00e−02	1.00e−02	1.36	1.36
133	Tyr	1.00e−02	6.78e−04	1.36	4.51
134	Glu	1.00e−02	8.94e−04	1.36	3.86
135	Phe	1.00e−02	7.01e−04	1.36	4.09
136	Glu	1.00e−02	7.24e−05	1.36	5.36
137	Ser	1.00e−02	3.97e−04	1.36	5.26
138	Ser	1.00e−02	1.00e−02	1.36	1.36
139	Glu	1.00e−02	4.32e−04	1.36	4.64
140	Ala	1.11e−03	1.00e−07	4.15	9.54
141	Val	4.29e−04	1.96e−06	3.97	7.16
142	Val	4.65e−04	2.45e−05	3.73	5.47
143	Asp	1.00e−02	1.00e−02	1.36	1.36
144	Gly	1.00e−02	1.00e−02	1.36	1.36
145	Lys	1.52e−03	7.70e−04	4.35	4.75
146	Phe	6.08e−04	1.00e−07	4.55	9.54
147	Val	2.59e−04	1.00e−07	4.35	9.54
148	Gly	5.83e−04	1.00e−07	4.92	9.54
149	Leu	3.00e−04	–	4.57	–
150	Ala	5.52e−04	1.00e−07	4.48	9.54
151	Leu	1.96e−04	1.00e−07	4.59	9.54
152	Asp	1.00e−02	1.00e−02	1.36	1.36
153	Leu	1.00e−02	1.70e−03	1.36	3.07
154	Asp	1.00e−02	1.00e−07	1.36	9.54
155	Asn	1.00e−02	3.29e−04	1.36	5.50
156	Gln	–	–	–	–
157	Ser	1.00e−02	1.00e−02	1.36	1.36
158	Gly	–	–	–	–
159	Lys	1.00e−02	1.00e−02	1.36	1.36
160	Thr	1.00e−02	1.00e−02	1.36	1.36
161	Asp	1.00e−02	1.00e−02	1.36	1.36
162	Glu	1.00e−02	1.00e−02	1.36	1.36
163	Arg	–	2.77e−05	–	6.45
164	Val	–	1.00e−07	–	9.54
165	Ala	2.27e−05	–	6.47	–
166	Ala	–	–	–	–
167	Trp	4.27e−06	1.00e−07	7.09	9.54
168	Leu	1.13e−06	1.00e−07	7.49	9.54
169	Ala	2.59e−06	1.00e−07	7.66	9.54
170	Gln	6.63e−06	1.00e−07	7.47	9.54
171	Ile	2.51e−06	1.00e−07	7.24	9.54
172	Ala	4.27e−06	1.00e−07	7.34	9.54
173	Pro	–	–	–	–
174	Glu	1.00e−02	1.81e−03	1.36	3.04
175	Phe	–	6.90e−06	–	6.83
176	Gly	–	–	–	–
177	Leu	8.04e−04	2.10e−03	3.99	3.42
178	Ser	1.00e−02	1.00e−02	1.36	1.36
179	Leu	1.00e−02	1.00e−02	1.36	1.36

For amide protons which exchanged so rapidly that they were not observed in our experiments in ^2H_2O, k_{ex} was set to 1.00 10^{-2} s^{-1} (and ΔG_{op} to 1.36 kcal mol^{-1}). For amide protons which had not exchanged in 42 h, $\log(k_{ex})$ was set to −7.00 (and ΔG_{op} to 9.54 kcal mol^{-1}). Part of the data were previously presented in Refs. [6,9]. A (–) indicates that the exchange rate could not be determined.

[16]. The incorporation of the flavin affects not only the flavin-binding region of the molecule but also extends to regions of the molecule distant from the bound flavin, as illustrated by the exchange behaviour of Val142.

Using the known dissociation constant for flavin release of *A. vinelandii* flavodoxin [17], the concentration free flavin in the NMR sample of holoflavodoxin is calculated to be 1.38 μM. The global stability of holoflavodoxin, ΔG(holo), is subsequently determined using the following equation:

$$\Delta G(\text{holo}) = \Delta G(\text{apo}) + RT\ln(1 + K_b * |FMN|), \quad (6)$$

in which K_b is the flavin-binding constant, and |FMN| is the equilibrium concentration of unbound flavin. Under the assumption that the global stability of apoflavodoxin, ΔG(apo),

equals the average ΔG_{op} value of the residues which are part of the stabilisation centre of apoflavodoxin ($\Delta G_{op} = 7.0$ kcal mol^{-1}), the global stability of holoflavodoxin is calculated to be $> \sim 11.8$ kcal mol^{-1}. This agrees with $\Delta G_{op} \geqslant \sim 9.5$ kcal mol^{-1} for the most slowly exchanging residues in holoflavodoxin.

Upon going from apo- to holoflavodoxin, the decrease in exchange rate of several residues of the stabilisation centre of holoflavodoxin exceeds a factor of 10,000. Other residues, e.g., Lys145 and Lys123, show a rather marginal decrease in exchange rate, 2.0 and 2.2 times, respectively. This demonstrates that the global stability increase does not simply transfer to a multiplication of the amide proton exchange rates of all residues of apoflavodoxin with a constant factor. The structural basis of the effects of ligand binding on exchange remains far from clear [16]. The amide proton exchange rates and local stabilities for a few amide protons of holoflavodoxin are similar within error to those measured for apoflavodoxin. Exchange of the amide protons of Arg24, Ala45, Gln46, Phe49, Leu84, Asp119, Lys123 and Lys145, therefore, takes place via local unfolding of holoflavodoxin and no global unfolding is required.

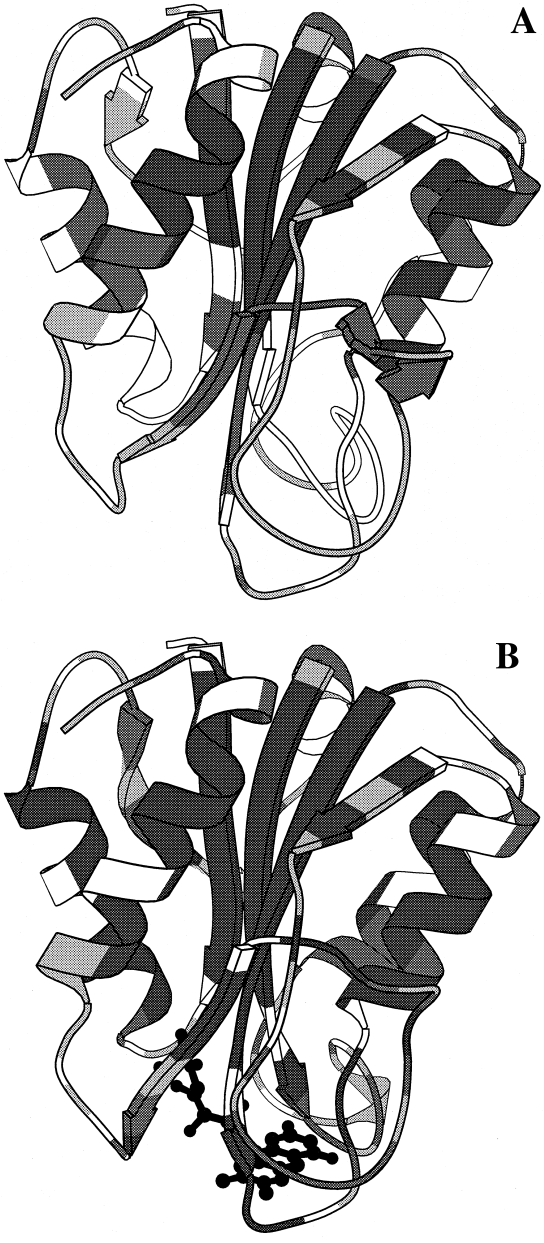

Fig. 4. Molscript cartoon drawing [21] of the X-ray structure of *A. chroococcum* flavodoxin [22]. The structure is grey-colored according to the calculated local stability differences for transient opening of the structure for the backbone amide protons of the highly homologous *A. vinelandii* apoflavodoxin (A) [9] and holoflavodoxin (B) [6] both in 150 mM potassium pyrophosphate, pH* 6.2 and 303 K. The most slowly exchanging amide protons reside in the ordered core of the molecule which is coloured dark grey and forms the stabilisation centre. Light grey: $\Delta G_{op} \leq 3.0$ kcal mol^{-1}; medium grey: 3.0 kcal mol^{-1} $< \Delta G_{op} <$ 6.2 kcal mol^{-1}; dark grey: $\Delta G_{op} \geq 6.2$ kcal mol^{-1}; white: proline residue or residue of which the amide proton could not be assigned by NMR spectroscopy or overlap of ^{1}H–^{15}N HSQC cross peaks. The length of the α-helices and of the β-strands shown in the global fold of apoflavodoxin [9] and of holoflavodoxin [6] are determined by the respective NMR data.

3.3. Stabilisation centres differ between structurally homologous proteins

The stabilisation centre of a protein is defined by us as the most stable part of a protein topology consisting of one or more secondary structure elements. In case of apoflavodoxin, it is shown that the stabilisation centre comprises residues in strands β1, β3, β4 and β5a and in helices α4 and α5. Incorporation of the FMN cofactor leads to a significant increase of the

local stabilities of the majority of the residues of apoflavodoxin. However, to be able to compare the inherent structure and inherent stability of flavodoxin with those of Che Y and cutinase, which are both members of superfamilies sharing the flavodoxin-like fold, the local stability values of apoflavodoxin have to be used. Both Che Y and cutinase are sequentially unrelated with flavodoxin. Whereas apoflavodoxin binds FMN and transfers electrons, the chemotactic protein Che Y binds a Mg^{2+} ion and transfers signals via phosphorylation, and the lipolytic enzyme cutinase degrades cutin and hydrolyses triglycerides. Just as is the case for apoflavodoxin; the hydrogen exchange characteristics and local stabilities of Che Y and of cutinase were determined in the absence of any cofactor [18,19].

As compared to apoflavodoxin, the amide exchange results show that both Che Y and cutinase have different stabilisation centres (Fig. 5). The most stable part of cutinase resides in strands β1, β2, β3 and β4 and in helices α2 and α3 ([18]; Prompers, personal communication). In contrast to what is found for apoflavodoxin and cutinase, all exchange rates of the slowly exchanging amide protons of Che Y show similar values slightly dispersed around a relatively low average value, as expected from its low stability [19]. Most of the protection from exchange are clustered on one face of the β-sheet of Che Y which is opposite to the side where the stability centre of cutinase is positioned (Fig. 5). The stable centres of structurally homologous proteins can thus reside in different parts of the same protein topology. If folding of these proteins is initiated with the collapse of the stabilisation centre as has been found for several other proteins, the folding pathways of structurally homologous proteins seem to be unrelated as well [9].

Knowledge about the stabilisation centres and the unstable regions of proteins is necessary to be able to rationally improve natural proteins to apply their function on an industrial scale. Knowledge about the unstable regions of a protein is also of relevance with respect to protein precipitation. Precipitation of proteins often results from the intermolecular interaction between specific exposed hydrophobic surfaces of partially unfolded molecules. Single amino acid substitutions in such regions can potentially suppress heat-induced aggregation without significantly affecting the other properties of the protein. The latter is of direct biotechnological relevance. The mutational strategy to be followed in case of proteins with a flavodoxin-like fold is to replace residues in the unstable regions with those of residues found in equivalent positions but with much higher local stability (Fig. 5). As has recently been demonstrated for a thermolysin-like protease from *Bacillus*

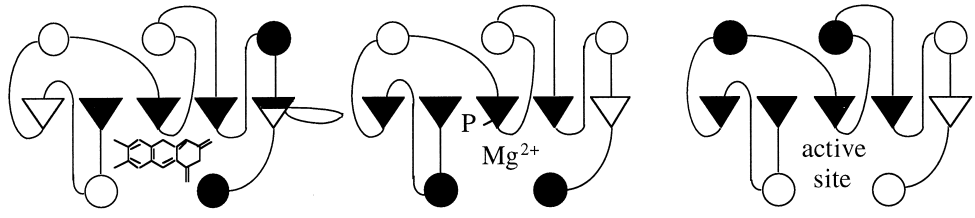

Fig. 5. Comparison of the stable parts in the topologies of three proteins which have no sequence homology but which share the flavodoxin-like fold. The secondary structure elements which contain the most slowly exchanging amide protons of: (1) apoflavodoxin at pH* 6.2 and 303 K [9], (2) Che Y at pH* 6.0 and 298 K [19] and (3) cutinase at pH 5.0 and 298 K ([18]; Prompers, personal communication) are depicted in black. An amino acid residue is element of the stable part of an individual protein species when it belongs to a continuous stretch of more than one residue with: (1) $\log P > 4.6$ for apoflavodoxin, (2) $\log P \geq 4.0$ for Che Y, and (3) $\log P \geq 6.0$ for cutinase. α-Helices are represented as circles, β-strands as triangles and loops as lines.

stearothermophilus, only a limited number of mutations are required to substantially stabilise an enzyme [20]. The key to success in case of the protease mentioned was insight in the (local) unfolding processes of the protein via an extensive mutation study [20]. As shown in this paper, hydrogen exchange measurements in combination with heteronuclear multidimensional NMR spectroscopy can circumvent the use of dozens of mutants. The unstable regions of a protein and its stabilisation centre are relatively straightforwardly determined using this methodology. The observation that stabilisation centres differ between structurally homologous proteins makes this methodology an extremely valuable tool in the search for stabilisation of proteins.

Acknowledgements

The research of Carlo P.M. van Mierlo was made possible by a fellowship of the Royal Netherlands Academy of Arts and Sciences.

References

[1] S.E. Brenner, Population statistics of protein structures: lessons from structural classifications, Curr. Opin. Struct. Biol. 7 (1997) 369.

[2] S.G. Mayhew, G. Tollin, General properties of flavodoxins. in: F. Müller (Ed.), Chemistry and Biochemistry of Flavoenzymes, Vol. 3, CRC Press, Boca Raton, FL, 1992, p. 389.

[3] M. Tanaka, M. Haniu, K.T. Yasunobu, D.C. Yoch, Complete amino acid sequence of azotoflavin, a flavodoxin from *Azotobacter vinelandii*, Biochemistry 16 (1977) 3525.

[4] E. Steensma, H.A. Heering, W.R. Hagen, C.P.M. van Mierlo, Redox properties of wild-type, Cys69Ala, and Cys69Ser *Azotobacter vinelandii* flavodoxin II as measured by cyclic voltammetry and EPR spectroscopy, Eur. J. Biochem. 235 (1996) 167.

[5] C.P.M. van Mierlo, P. Lijnzaad, J. Vervoort, F. Müller, H.J.C. Berendsen, J. de Vlieg, Tertiary structure of two-electron reduced *Megasphaera elsdenii* flavodoxin and some implications, as determined by two-dimensional ^{1}H-NMR and restrained molecular dynamics, Eur. J. Biochem. 194 (1990) 185.

[6] E. Steensma, M.J.M. Nijman, Y.J.M. Bollen, P.A. de Jager, W.A.M. van den Berg, W.M.A.M. van Dongen, C.P.M. van Mierlo, Apparent local stability of the secondary structure of *Azotobacter vinelandii* holoflavodoxin II as probed by hydrogen exchange: implications for redox potential regulation and flavodoxin folding, Protein Sci. 7 (1998) 306.

[7] S.S. Wijmenga, E. Steensma, C.P.M. van Mierlo, Doubly sensitivity-enhanced 3D HCCH-TOCSY of ^{13}C-labelled proteins in H_2O using heteronuclear cross polarization and pulsed field gradients, J. Magn. Reson. 124 (1997) 459.

[8] S.S. Wijmenga, C.P.M. van Mierlo, E. Steensma, Doubly sensitivity-enhanced 3D TOCSY-HSQC, J. Biomol. NMR 8 (1996) 319.

[9] E. Steensma, C.P.M. van Mierlo, Structural characterisation of apoflavodoxin shows that the location of the most stable nucleus differs among proteins with a flavodoxin-like topology, J. Mol. Biol. 282 (1998) 653.

[10] S.W. Englander, N.R. Kallenbach, Hydrogen exchange and structural dynamics of proteins and nucleic acids, Q. Rev. Biophys. 16 (1984) 521.

[11] C.P.M. van Mierlo, W.M.A.M. van Dongen, F. Vergeldt, W.J.H. van Berkel, E. Steensma, The equilibrium unfolding of *Azotobacter vinelandii* apoflavodoxin II occurs via a relatively stable folding intermediate, Protein Sci. 7 (1998) 2331.

[12] D.E. Edmondson, G. Tollin, Chemical and physical characterisation of the Shethna flavoprotein and apoprotein and kinetics and thermodynamics of flavin analog binding to the apoprotein, Biochemistry 10 (1971) 124.

[13] K. Linderstrøm-Lang, Deuterium exchange between peptides and water, Chem. Soc. (London) 2 (1955) 1, Spec. Publ.

[14] A. Hvidt, S.O. Nielsen, Hydrogen exchange in proteins, Adv. Protein Chem. 21 (1966) 287.

[15] Y. Bai, J.S. Milne, L. Mayne, S.W. Englander, Primary structure effects on peptide group hydrogen exchange, Proteins Struct. Funct. Genet. 17 (1993) 75.

[16] C. Woodward, I. Simon, E. Tüchsen, Hydrogen exchange and the dynamic structure of proteins, Mol. Cell. Biochem. 48 (1982) 135.

[17] J.J. Pueyo, G.P. Curley, S.G. Mayhew, Kinetics and thermodynamics of the binding of riboflavin, riboflavin 5′-phosphate and riboflavin 3′,5′-bisphosphate by apoflavodoxins, Biochem. J. 313 (1996) 855.

[18] J.J. Prompers, A. Groenewegen, R.C. van Schaik, H.A.M. Pepermans, C.W. Hilbers, ^{1}H, ^{13}C and ^{15}N resonance assignments of *Fusarium solani pisi* cutinase and preliminary features of the structure in solution, Protein Sci. 6 (1997) 2375.

[19] E. Lacroix, M. Bruix, E. López-Hernández, L. Serrano, M. Rico, Amide hydrogen exchange and internal dynamics of the chemotactic protein Che Y from *Escherichia coli*, J. Mol. Biol. 271 (1997) 472.

[20] B. van den Burg, G. Vriend, O.R. Veltman, G. Venema, V.G.H. Eijsink, Engineering an enzyme to resist boiling, Proc. Natl. Acad. Sci. USA 95 (1998) 2056.

[21] P.J. Kraulis, MOLSCRIPT: a program to produce both detailed and schematic plots of protein structures, J. Appl. Cryst. 24 (1991) 946.

[22] R.N.F. Thorneley, G.A. Ashby, M.H. Drummond, R.R. Eady, D.L. Hughes, G. Ford, P.M. Harrison, A. Shaw, R.L. Robson, J. Kazlauskaite, H.A.O. Hill, Flavodoxins and nitrogen fixation-structure, electrochemistry and post-translational modification by coenzyme A, in: K. Yagi (Ed.), Flavins and Flavoproteins 1993, Walter de Gruyter, Berlin, 1994, p. 343.